ACS APPLIED MATERIALS & INTERFACES

Research Article

www.acsami.org

TEMPO/Viologen Electrochemical Heterojunction for Diffusion-Controlled Redox Mediation: A Highly Rectifying Bilayer-Sandwiched Device Based on Cross-Reaction at the Interface between Dissimilar Redox Polymers

Hiroshi Tokue, Kenichi Oyaizu,* Takashi Sukegawa, and Hiroyuki Nishide*

Department of Applied Chemistry, Waseda University, Tokyo 169-8555, Japan

Supporting Information

ABSTRACT: A couple of totally reversible redox-active molecules, which are different in redox potentials, 2,2,6,6-tetramethylpiperidin-1-oxyl (TEMPO) and viologen (V^{2+}), were employed to give rise to a rectified redox conduction effect. Single-layer and bilayer devices were fabricated using polymers containing these sites as pendant groups per repeating unit. The devices were obtained by sandwiching the redox polymer layer(s) with indium tin oxide (ITO)/glass and Pt foil electrodes. Electrochemical measurements of the single-layer device composed of polynorbornene-bearing TEMPO (PTNB) exhibited a diffusion-limited current−voltage response based on the $TEMPO^+$/TEMPO exchange reaction, which was almost equivalent to a redox gradient through the PTNB layer depending upon the thickness. The bilayer device gave rise to the current rectification because of the thermodynamically favored cross-reaction between $TEMPO^+$ and V^+ at the polymer/polymer interface. A current−voltage response obtained for the bilayer device demonstrated a two-step diffusion-limited current behavior as a result of the concurrent V^{2+}/V^+ and V^+/V^0 exchange reactions according to the voltage and suggested that the charge transport process through the device was most likely to be rate-determined by a redox gradient in the polymer layer. Current collection experiments revealed a charge transport balance throughout the device, as a result of the electrochemical stability and robustness of the polymers in both redox states.

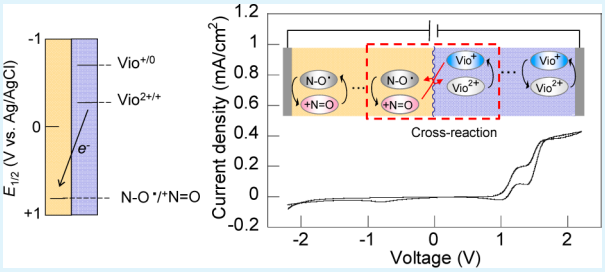

KEYWORDS: *charge transport, rectification, redox polymer, heterojunction, self-exchange reaction, bilayer*

INTRODUCTION

Charge transport processes with redox mediation by various types of redox-active layers dominate the performance of electrochemical devices, such as dye-sensitized solar cells (DSSCs),[1−7] electrochromic displays,[8−10] (bio)sensors,[11−13] and light-emitting electrochemiluminescent devices.[14−18] Current density obtained by the redox-mediated processes are the most important factors to determine the performance of the electrochemical devices,[19−21] and for this purpose, a number of redox-active species have been examined, such as ferrocene,[22−24] triphenylamine,[25,26] anthraquinone[27,28] and viologen,[29,30] taking advantage of their large rate constants for the heterogeneous electron transfer process at electrode interfaces.[31] However, the mediation current has often been limited by self-exchange and cross-reaction processes in redox-active layers, which have impeded studies upon further development of novel electrochemical cells.

A breakthrough recently made by our group in the area of the electrochemical devices is the finding that polymers containing organic robust radicals, such as 2,2,6,6-tetramethylpiperidin-1-oxyl (TEMPO),[32−38] 2,2,5,5-tetramethyl-1-pyrrolidinoxy (PROXYL),[39,40] galvinoxyl,[41,42] and nitronyl nitroxide,[43,44] per repeating unit undergo reversible charging and discharging, with the amount of charge comparable to their formula-weight-based theoretical charge-storage densities. Such properties of the so-called radical polymers have been focused on the development of an entirely organic battery with a large energy density and an excellent power-rate capability.[45−47]

We anticipated that an ideal redox mediation process, allowing for large current densities, should be accomplished with a single-layer device composed of the radical polymer based on the facile charging/discharging process of the polymer layer attached to a current collector. Moreover, the theoretically matched charge-storage density[48] suggested that the diffusion front traveled throughout the polymer layer on the current collector to fully equilibrate the redox state up to the outer surface (i.e., the polymer/electrolyte interface) of the layer, which inspired us to develop a rectifying process by placing a cross-reaction at the interface. In this report, the radical polymers are characterized as efficient redox mediators, giving rise to not only a diffusion-limited charge transport process but also a rectification effect, by fabricating polymer-sandwiched

Received: December 3, 2013
Accepted: February 21, 2014
Published: February 21, 2014

thin-layer devices. Emphasis is placed on the finding that a TEMPO-substituted polynorbornene and a polypyrrole-based viologen polymer (Figure 1) both formed fully redox-active

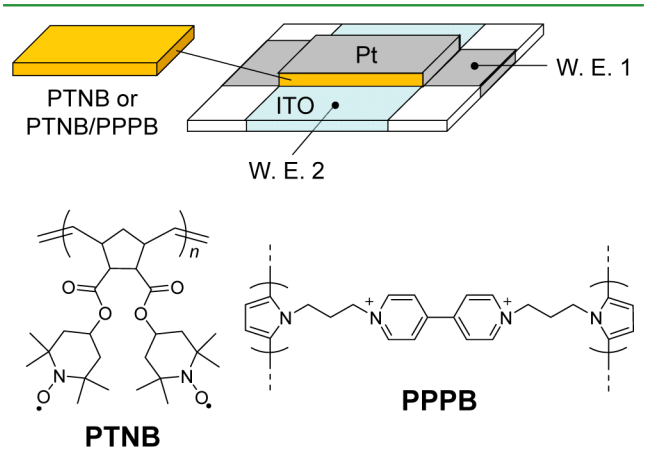

Figure 1. Schematic representation of single-layer and bilayer devices, illustrating the arrangement of the two working electrodes. The working potentials were scanned independently, with respect to the Ag/AgCl reference electrode in a four electrode system. W. E. 1, first working electrode; W. E. 2, second working electrode.

thin layers with precisely tunable thickness[1,48] and the chemically reactive outer surfaces.[2] The rectified diffusion-limited "redox conduction" based on the thermodynamically favored cross-reaction at polymer/polymer interfaces gave insight into the nature of the photovoltaic effect in dye-sensitized solar cells[1] and related biological processes, such as photosynthesis and respiratory systems.

EXPERIMENTAL SECTION

Materials. Sodium dithionite was purchased from Junsei Chemical. 2,6-Bis(*p*-azidobenzal)-4-*tert*-amylcyclohexanone was purchased from Tokyo Gosei. All other reagents were purchased from Sigma-Aldrich and used without further purification. All solvents were distilled for purification before use. The indium tin oxide (ITO)/glass electrode was purchased from Asahi Glass, which was cleaned by plasma etching before use.

Apparatus. ^{1}H and ^{13}C nuclear magnetic resonance (NMR) spectra were recorded on a JEOL JNM-LA 500 spectrometer with chemical shifts downfield from tetramethylsilane as an internal standard. Infrared spectra were obtained using a JASCO FT/IR-6100 spectrometer. Ultraviolet−visible (UV−vis) spectra were recorded using an ALS spectrometer SEC 2000. Mass spectra were obtained using a JEOL JMS-SX 102A spectrometer or a Shimadzu GCMS-QP5050 spectrometer. Electrospray ionization mass spectrometry (ESI−MS) spectroscopy was performed for the negative-ion mode using the ion-trap Thermo Quest Finnigan LCQ Deca. Elemental analyses were performed using a Perkin-Elmer model PE-2400 II elemental analyzer and a Metrohm model 645 Multi-Dosimat auto buret. Two parallel analyses were performed for each sample. Molecular weight measurements were performed by gel permeation chromatography using a TOSOH HLC 8220 instrument with tetrahydrofuran as the eluent. Electron spin resonance (ESR) spectra were recorded using a JEOL JES-TE200 spectrometer with a 100 kHz field modulation and a 0.1 mT width. The film thicknesses were estimated using a KLA Tencor P-6 contact stylus profiler.

Electrochemical Measurements. Electrochemical analyses were carried out using an ALS electrochemical analyzer 760 EW. All analyses were performed under nitrogen. A coiled platinum wire or a glassy carbon plate (2.5 × 2.5 cm) was employed as a counter electrode, and a commercial Ag/AgCl immersed in a solution of 0.1 M $TBAClO_4$ in CH_3CN was employed as a reference electrode. The formal potential of the ferrocene/ferrocenium couple was +0.45 V versus this Ag/AgCl electrode. Diffusion coefficients D_e for the redox gradient-driven charge transport process in polymer layers were determined from the slope of Cottrell plots obtained from potential-step chronoamperometry according to $i = nFAC_T(D_e/\pi t)^{1/2}$, where n, A, and C_T are the number of electrons, the working electrode area, and the concentration of the pendant redox site, respectively.

Preparation of a Photo-cross-linked Poly[2,3-bis(2′,2′,6′,6′-tetramethylpiperidin-1′-oxyl-4′-oxycarbonyl)-5-norbornene] (PTNB) Electrode. The photo-cross-linked PTNB electrode was prepared by a procedure described in the literature,[48] with slight modification as follows. The norbornene monomer bearing TEMPO as redox-active site was synthesized from *cis*-5-norbornene-*endo*-2,3-dicarboxylic anhydride. The corresponding polymer was obtained by conventional ring-opening metathesis polymerization of the monomer (M_n = 23 700; M_w/M_n = 1.3). To an ethyl lactate solution of PTNB (42−91 mg, 7.5−15 wt %) was added a toluene solution of a photo-cross-linker, 2,6-bis(*p*-azidobenzal)-4-*tert*-amylcyclohexanone (3.2−6.9 mg, 7.5−15 wt %), and the mixture was spin-coated on an ITO substrate using a Mikasa 1H-D3 spin coater at 800−2000 rpm. After drying in vacuum for 12 h, photo-cross-linking was carried out by UV irradiation (40 mJ/cm^2, USH-250D, Ushio, Inc.). Finally, the polymer electrode was washed with acetonitrile to remove any soluble part.

Preparation of a Poly[*N*,*N*′-bis(3-pyrrole-1-yl-propyl)-4,4′-bipyridinium] (PPPB) Electrode. *N*,*N*′-Bis(3-pyrrole-1-yl-propyl)-4,4′-bipyridinium ditetrafluoroborate was synthesized and eletropolymerized according to the method described in a previous report.[49] The pyrrole monomer containing the viologen was synthesized via the Clauson-Kaas reaction using 3-bromopropylamine and 2,5-dimethyltetrahydrofuran as starting materials and the Menschutkin reaction with 4,4′-bipyridyl. PPPB films were electropolymerized for 2−40 min onto an ITO substrate from 0.1 M Bu_4NClO_4/CH_3CN with the 2 mM pyrrole monomer, by maintaining the electrode potential at +1.25 V versus Ag/AgCl using a glassy carbon substrate as a counter electrode. The film thickness of PPPB was proportional to the charge passed during the electropolymerization.

Synthesis of *N*,*N*′-Dimethyl-4,4′-bipyridinium hexafluorophosphate ($MV^+PF_6^-$). *N*,*N*′-Dimethyl-4,4′-bipyridinium, commonly referred to as methylviologen (MV), and a hexafluorophosphate salt of a one-electron-reduced cation radical ($MV^+PF_6^-$) was synthesized according to previous literature.[50] $MV^+PF_6^-$ was prepared via the reduction of $[MV^{2+}]Cl_2$ by sodium dithionite, followed by an anion-exchange process. All processes were performed under an argon atmosphere.

Synthesis of Tetrafluoroborate Salt of TEMPO$^+$. Synthesis of a tetrafluoroborate salt of $TEMPO^+$ ($TEMPO^+BF_4^-$) has been reported by our group.[51] $TEMPO^+BF_4^-$ was prepared via the oxidation of TEMPO by sodium hypochlorite in the presence of tetrafluoroboric acid.

Fabrication of Single-Layer and Bilayer Devices. Both single-layer and bilayer devices were fabricated by sandwiching the polymer layer(s) between ITO/glass and Pt. A part of the ITO/glass was etched with aqua regia vapor for 30 min, and the etched part was washed with pure water. The etched ITO was then sequentially sonicated in acetone, pure water, Semico Clean (Furuuchi Chemical), and isopropyl alcohol for 30 min. PTNB film was spin-coated on the etched ITO for the single-layer device. For the bilayer device, PPPB was electropolymerized on the etched ITO and then photo-cross-linked PTNB was laminated on the PPPB layer. Next, pure water was dropped on the photo-cross-linked PTNB single-layer or photo-cross-linked PTNB/PPPB laminated layer, and Pt foil was placed on the wet polymer. Then, the pure water was removed by vacuum drying for 12 h to obtain a polymer/Pt interface.

Potential Control and Cell Arrangement. Four-electrode configuration allowing for independent control of the potentials for the two working electrodes relative to the reference electrode was employed to obtain a current−potential response from the sandwiched devices (Figure 1). A Pt foil was employed as the first working electrode, and its potential (E_{Pt}) was scanned. An ITO/glass plate was employed as the second working electrode, and its potential (E_{ITO})

was fixed. The current at each of the Pt and ITO electrodes was measured as a function of the electrode potentials. A two-electrode system was also used for examination of the current−voltage response from the bilayer device, where ITO was employed as the working electrode and Pt was employed as the counter and reference electrodes. The current between the ITO and Pt electrodes was measured as a function of the voltage applied to the device.

RESULTS AND DISCUSSION

Cyclic voltammograms obtained for the layers of photo-cross-linked PTNB and PPPB are shown in Figure 2. The PTNB

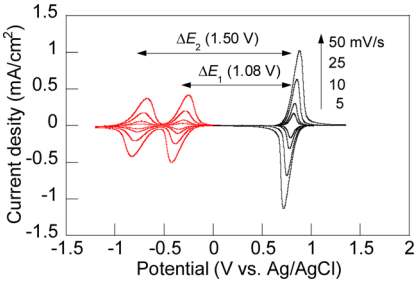

Figure 2. Cyclic voltammograms obtained for the layers of photo-cross-linked PTNB (black solid curve) and PPPB (red solid curve) in 0.1 M $(CH_3)_4NClO_4$ in acetonitrile at a scan rate of v = 5, 10, 25, and 50 mV/s. ΔE represents the potential gap between the two polymers. ΔE_1 and ΔE_2 correspond to the gaps for the first ($E_{1/2}$ = −0.28 V) and second ($E_{1/2}$ = −0.70 V) redox reactions of PPPB, respectively. Thicknesses of the polymer layers were 70 nm for photo-cross-linked PTNB and 90 nm for PPPB.

layer exhibited a reversible redox response at $E_{1/2}$ = +0.81 V versus Ag/AgCl, which was ascribed to a one-electron oxidation of the TEMPO unit. The PPPB layer exhibited a two-step wave at $E_{1/2}$ = −0.28 and −0.70 V, because of the reductions of the viologen (V^{2+}) group to produce the cation radical V^+ and then the neutral V^0 groups per repeating unit. Each of the anodic and cathodic peak current densities and their amounts of charge obtained by integration of the voltammetric waves were equal, which suggested the electrochemical reversibility of the redox reactions and chemical stability of all of the redox states involved in both polymers. The peak current densities were proportional to the potential scan rate v as a result of the fast charge propagation in the thin layers to represent the Nernstian absorbate-like behavior,[32] indicative of the surface-confined electrochemical process. Narrow peak-to-peak separations (i.e., 32 mV for the layer of photo-cross-linked PTNB and 42 and 24 mV for the first and the second waves of PPPB, respectively) demonstrated rapid charge transport in the polymer layers. Negligible diffusion tails revealed that all of the redox sites in the polymers readily responded to the electrode potential, even for those placed away from the electrode surface with a distance of 70−90 nm, because of the rapid charge transport. It may be noted that the potential gap between the two polymers was so large (ΔE_1 = 1.08 V, and ΔE_2 = 1.50 V) (Figure 2) that the cross-reaction at the polymer/polymer interface should be sufficiently favored to give rise to the rectification effect of the bilayer device (*vide infra*).

Cyclic voltammograms of the photo-cross-linked PTNB single-layer device were recorded with the four-electrode circuitry (Figure 1) to reveal the excellent performance of the polymer layer as the charge transport media. Both anodic and cathodic currents increased at the redox potential of the polymer and then reached a plateau (Figure 3).

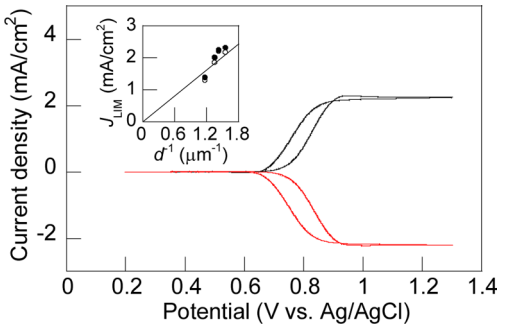

Figure 3. Four-electrode cyclic voltammograms obtained for the photo-cross-linked PTNB single-layer device in 0.1 M $(CH_3)_4NClO_4$ in acetonitrile, showing both first working (Pt) (black solid curve) and second working (ITO) (red solid curve) electrode current densities. The thickness of the polymer layer was 700 nm. E_{ITO} was maintained at 0 V, and E_{Pt} was scanned from +0.2 to +1.3 V at 5 mV/s. The inset shows anodic (●) and cathodic (○) diffusion-limited current density J_{LIM} versus the inverse of the PTNB layer thickness d^{-1}.

The current flow process in the single-layer device consisted of the electrode reaction and the charge transport through the polymer layer. The presence of the plateau current indicated that the electrode reaction was so fast that it did not determine the current through the photo-cross-linked PTNB layer and that the diffusion-limited charge transport throughout the polymer layer with 700 nm in thickness was accomplished at the sufficiently large overpotentials. In redox polymers, charge transport is driven by an electron self-exchange reaction between adjacent redox sites and dominated by a diffusion of charge based on the redox gradient produced under the electrolyte conditions. When the anode potential is more positive and the cathode potential is more negative than $E_{1/2}$ of the sandwiched polymer, a steady-state redox gradient through the polymer layer is maximized (Figure 4).

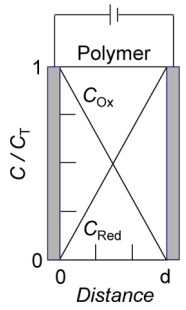

Figure 4. Steady-state concentration gradients of oxidized and reduced species through the single-layer device at a sufficient bias voltage.

The redox gradient provides the diffusion-limited current density J_{LIM} obtained for the sandwich device according to the following equation:[52]

$$J_{LIM} = \frac{\omega^0 nFD_e C_T}{d} \quad (1)$$

where n, F, C_T, and d are the number of electrons, the Faraday constant, the concentration of the pendant redox site, and the polymer thickness, respectively. ω^0 is a correction factor for an electrostatic coupling between electron and counterion motion. The values of ω^0 for the redox reactions of photo-cross-linked PTNB and PPPB were calculated to be 1.50 and 1.11,

respectively, according to the theory described in the literature[53] (for evaluation of D_e, see the Experimental Section). The diffusion coefficient D_e reflected the mass transfer process for the electroneutralizing ions during the electrochemical exchange reaction in the layer. The observed J_{LIM} in Figure 3 (2.3 mA/cm^2) coincided with the theoretical value for the PTNB single-layer device (2.5 mA/cm^2). It may be noted that J_{LIM} obtained with the polymers in different thicknesses was proportional to d^{-1} according to eq 1 (Figure 3). These results demonstrated that the charge transport was ideally driven by the concentration gradient formed as a function of the charge transport distance in the device. This ideal property of the charge transport process indicated that the polymer layer was almost defect-free as a result of the amorphous and non-conjugated structure of the radical polymer to provide the uniform charge propagation medium throughout the layer. Moreover, the contact stylus profile obtained for the PTNB and PPPB layers revealed flat surfaces with a roughness of less than 6 and 15 nm, respectively (see Figure S1 of the Supporting Information), which promised a constant charge transport distance between the two electrodes of the device. Figure 3 showed a small hysteresis in currents between the forward and backward scans, as a result of transient response from the diffusion-limited layer.

The cyclic voltammogram also displayed simultaneous increases of anodic and cathodic currents according to the potential scan, which was illustrative of the rapid charge transport through the polymer layer. Moreover, almost the same magnitudes of anodic and cathodic currents J_{LIM} suggested the robustness of the photo-cross-linked PTNB in both redox states to allow for a highly balanced charge transport. Current−voltage response obtained for the single-layer device displayed a sigmoidal curve and diffusion-limited currents at both positive and negative voltages (see Figure S2 of the Supporting Information). The result supported that the charge transport was dominated by the redox gradient and was varied as a function of the bias voltage.

The polymer layers were preconditioned by repeated potential scanning to incorporate electrolyte ions and solvents, so that the mass transfer process to yield the steady-state current was most likely dominated by the redistribution of the electroneutralizing ions already accommodated in the layer rather than the inclusion and exclusion of the electrolyte ions at the edge of the sandwiched device.

The electrochemical response from the polymer/Pt foil as the working electrode, obtained with the Pt wire and Ag/AgCl as the auxiliary and reference electrodes (see Figure S3 of the Supporting Information), revealed the amount of charge equivalent to the formula-weight-based theoretical redox density of the PPPB layer, which demonstrated the robustness of the mechanically placed Pt foil on the polymer layer.

The redox conduction effect incorporated a cross-reaction at the interface of dissimilar polymers, when the sandwiched layer was replaced with the bilayer of TEMPO and V^{2+} (see the Experimental Section for the fabrication of the bilayer device). Applying a forward voltage to the bilayer device gave rise to the interfacial cross-reaction according to eq 2

$$V^+ + TEMPO^+ \rightarrow V^{2+} + TEMPO \quad (2)$$

which was thermodynamically favored because of the large potential gap. The cross-reaction between V^+ and $TEMPO^+$ was examined by UV−vis spectral changes, using a chloride salt of *N*,*N*′-dimethyl-4,4′-bipyridinium (MV^{2+}) as a model compound for V^{2+} (see Figure S4a of the Supporting Information). Absorptions at 396 and 606 nm attributed to MV^+, prepared by electrolytic exhaustive reduction of MV^{2+}, readily disappeared with the addition of $TEMPO^+$, and no unidentified absorption appeared after the elimination of MV^+, which revealed that the cross-reaction went to completion without side reactions. The products of the cross-reaction, MV^{2+} and TEMPO, showed no significant absorption in the region of 300−800 nm. The absorption attributed to MV^+ was maintained when TEMPO was used instead of $TEMPO^+$ (see Figure S4b of the Supporting Information), which confirmed that V^+ was stable against TEMPO. ESR spectral changes recorded for MV^+ in dichloromethane with the addition of $TEMPO^+$ (see Figure S5 of the Supporting Information) revealed that a multimodal signal at g = 2.0030 because of MV^+ disappeared and then was replaced with a trimodal signal at g = 2.0062 because of the reduction of $TEMPO^+$ to yield TEMPO. The cross-reaction to dominate the redox conduction effect of the bilayer device was thus considered to be highly selective.

Current−voltage response obtained for the bilayer device composed of the photo-cross-linked PTNB and PPPB layers exhibited a rectified conduction effect. The rectification ratio, which is defined as the ratio of peak currents obtained at a given potential bias, was 16 at ±1.8 V in the bilayer device (Figure 5).

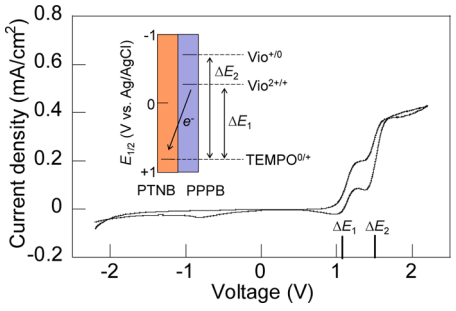

Figure 5. Two-electrode cyclic voltammogram obtained for the bilayer device composed of photo-cross-linked PTNB and PPPB in 0.1 M $(CH_3)_4NClO_4$ in acetonitrile at a scan rate of v = 5 mV/s. The thickness of the polymer layers was 700 nm for the two polymers.

Although the current density was relatively low, the ratio was comparable to the electrochemical diodes reported in previous literature.[54,55] It may be added that the ratio was lower than those obtained for other conventional devices,[56,57] but the current density for the present device surpassed those for the highly rectifying devices, as a result of the facile charge transport in the two layers (*vide infra*). Previous studies on the electrochemical rectifying devices were mainly based on the use of ionic conducting polymers[55,56] and self-doped conjugated polymers,[54,57] where increasing the rectification ratio yet maintaining the current density was a topic of issue. The present PTNB/PPPB device is characterized by the remarkable rectifying response to combine these properties at moderate levels. Driving voltages of the bilayer device corresponded to ΔE_1 and ΔE_2, which was suggestive of the presence of the cross-reaction at the polymer/polymer interface and indicated the possibility of tuning the driving voltage of the bilayer device by the potential gap between the two polymers. The wet process for the device fabrication allowed for close contact of the dissimilar layers, with 700 nm in thickness and the surface roughness of several nanometers.

The redox conduction effect by the bilayer device was dominated by both the cross-reaction and the exchange reaction through the polymer layers.[58,59] The overall current densities at sufficiently large overvoltages were determined by the exchange reaction. The current−voltage response displayed two distinct plateau currents (Figure 5), which suggested that two steady-state redox gradients formed in response to the applied voltage. Redox gradients of $V^{2+/+}$ and $TEMPO^{0/+}$ were formed through each layer in the voltage region, where the first plateau was observed. Theoretical J_{LIM} calculated from eq 1 was 2.5 mA/cm^2 for the photo-cross-linked PTNB layer and 0.34 mA/cm^2 for the PPPB layer, while the observed J_{LIM} in Figure 5 was 0.20 mA/cm^2. The good coincidence between the value of J_{LIM} for the bilayer device and that for pristine PPPB clearly demonstrated that the redox gradient through the PPPB layer determined the overall current. It may be added that the small deviation of the observed J_{LIM} from the calculational value would have been caused by the limitations in evaluating D_e and the swollen film thickness. The two-electron reduced V^0 produced at a higher voltage region changed the steady-state redox gradient to give rise to the second plateau current. The second J_{LIM} was larger than the first J_{LIM}, as a result of the faster charge diffusion based on the second redox reaction of viologen (D_e = 1.1 and 4.8 × 10^{-10} cm^2/s for the first and second reactions, respectively). The electron diffusivity D_e for the PPPB layer gave exchange rate constants of k_{ex} = 3.7 × 10^4 and 9.1 × 10^4 M^{-1} s^{-1} for the first and second reductions, respectively, which were comparable to those (8.4 × 10^3 and 1.6 × 10^5 M^{-1} s^{-1}) reported under different conditions.[49]

Cyclic voltammograms of the bilayer device recorded when the potential of the PPPB electrode was maintained at −1.2 V versus Ag/AgCl are shown in Figure 6.

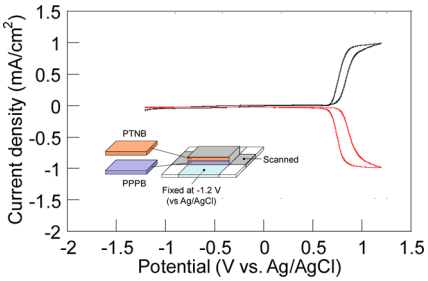

Figure 6. Four-electrode cyclic voltammogram obtained for the bilayer device composed of photo-cross-linked PTNB (300 nm) and PPPB (300 nm) in 0.1 M $(CH_3)_4NClO_4$ in acetonitrile, showing both first working (Pt) (black solid curve) and second working (ITO) (red solid curve) electrode current densities. $E_{W2\ (ITO)}$ was maintained at −1.2 V, and $E_{W1\ (Pt)}$ was scanned from −1.2 to +1.2 V at 2 mV/s.

The currents increased at the redox potential of the photo-cross-linked PTNB layer and then reached the plateau, as expected. Rapid charge transport, including the cross-reaction process, was demonstrated by the simultaneous increase of anodic and cathodic currents according to the potential scan. The equivalent diffusion-limited currents proved the balanced charge transport through the bilayer device, although the charges must undergo several processes to travel through the device.

Thinner layers of polymers, which exhibit charge transport based on the ideal redox mediation as described in this paper, are expected to provide larger current densities, because of steeper redox gradients. Further increasing the current density by reducing the layer thickness in the bilayer device down to <100 nm to exhibit the surface-confined process (Figure 2) while maintaining the rectification ratio of the device, which has thus far been impeded by the inherent surface roughness of the PPPB layer, is the topic of our continuous research.

CONCLUSION

The photo-cross-linked PTNB and PPPB layers coated on the current collector exhibited entirely reversible redox behaviors and rapid conversion of the redox state throughout the layers toward the equilibrium state established by electrode potentials. A single-layer device composed of the photo-cross-linked PTNB layer showed the diffusion-limited charge transport driven by the redox gradient depending upon the layer thickness as a result of the charge propagation through the homogeneous polymer layer. The rectified effect was obtained from the bilayer device fabricated by sandwiching the photo-cross-linked PTNB and PPPB layers with electrodes. Driving voltages of the bilayer device agreed with the redox potential gap between the two polymers, which suggested that the thermodynamically favored cross-reaction dominated the electrochemical response. Charge transport based on the ideal redox mediation in both layers allowed for rectified diffusion-controlled redox conduction, which was demonstrated by the current−voltage response corresponding to the redox gradient.

ASSOCIATED CONTENT

Supporting Information

Synthetic procedures, additional device performances, and spectroscopic results. This material is available free of charge via the Internet at http://pubs.acs.org.

AUTHOR INFORMATION

Corresponding Authors

*E-mail: oyaizu@waseda.jp.
*E-mail: nishide@waseda.jp.

Notes

The authors declare no competing financial interest.

ACKNOWLEDGMENTS

This work was partially supported by Grants-in-Aid for Scientific Research (24108739, 24225003, 24750113, 25107733, and 25288056) from the Ministry of Education, Culture, Sports, Science and Technology (MEXT), Japan.

REFERENCES

(1) Nishide, H.; Oyaizu, K. Toward flexible batteries. *Science* **2008**, *319*, 737−738.
(2) Kato, F.; Kikuchi, A.; Okuyama, T.; Oyaizu, K.; Nishide, H. Nitroxide radicals as highly reactive redox mediators in dye-sensitized solar cells. *Angew. Chem., Int. Ed.* **2012**, *51*, 10177−10180.
(3) Kinoshita, T.; Dy, J. T.; Uchida, S.; Kubo, T.; Segawa, H. Wideband dye-sensitized solar cells employing a phosphine-coordinated ruthenium sensitizer. *Nat. Photonics* **2013**, *7*, 535−539.
(4) Morita, S.; Wei, T.-C.; Ikegami, M.; Miyasaka, T. Tri-functional Nb_2O_5 nano-islands coated on an indium tin oxide layer for a highly efficient dye-sensitized plastic photoanode. *J. Power Sources* **2013**, *240*, 753−758.
(5) Yella, A.; Lee, H.-W.; Tsao, H. N.; Yi, C.; Chandiran, A. K.; Nazeeruddin, M. K.; Diau, E. W.-G.; Yeh, C.-Y.; Zakeeruddin, S. M.; Grätzel, M. Porphyrin-sensitized solar cells with cobalt (II/III)-based redox electrolyte exceed 12 percent efficiency. *Science* **2011**, *334*, 629−634.

(6) Nakashima, T.; Satoh, N.; Albrecht, K.; Yamamoto, K. Interface modification on TiO_2 electrode using dendrimers in dye-sensitized solar cells. *Chem. Mater.* **2008**, *20*, 2538−2543.
(7) Daeneke, T.; Kwon, T.-H.; Holmes, A. B.; Duffy, N. W.; Bach, U.; Spiccia, L. High-efficiency dye-sensitized solar cells with ferrocene-based electrolytes. *Nat. Chem.* **2011**, *3*, 211−215.
(8) Takahashi, Y.; Hayashi, N.; Oyaizu, K.; Honda, K.; Nishide, H. Totally organic polymer-based electrochromic cell using TEMPO-substituted polynorbornene as a counter electrode-active material. *Polym. J. (Tokyo, Jpn.)* **2008**, *40*, 763−767.
(9) Beaujuge, P. M.; Amb, C. M.; Reynolds, J. R. Spectral engineering in π-conjugated polymers with intramolecular donor−acceptor interactions. *Acc. Chem. Res.* **2010**, *43*, 1396−1407.
(10) Vasilyeva, S. V.; Beaujuge, P. M.; Wang, S.; Babiarz, J. E.; Ballarotto, V. W.; Reynolds, J. R. Material strategies for black-to-transmissive window-type polymer electrochromic devices. *ACS Appl. Mater. Interfaces* **2011**, *3*, 1022−1032.
(11) Chaubey, A.; Malhotra, B. D. Mediated biosensors. *Biosens. Bioelectron.* **2002**, *17*, 441−456.
(12) Spires, J. B.; Peng, H.; Williams, D. E.; Wright, B. E.; Soeller, C.; Travas-Sejdic, J. The effect of the oxidation state of a terthiophene-conducting polymer and of the presence of a redox probe on its gene-sensing properties. *Biosens. Bioelectron.* **2008**, *24*, 934−939.
(13) Huang, J.; Wrighton, M. S. Microelectrochemical multitransistor devices based on electrostatic binding of electroactive anionic metal complexes in protonated poly(4-vinylpyridine): Devices that can detect and distinguish up to three species simultaneously. *Anal. Chem.* **1993**, *65*, 2740−2746.
(14) Lai, R. Y.; Bard, A. J. Electrogenerated chemiluminescence. 70. The application of ECL to determine electrode potentials of tri-*n*-propylamine, its radical cation, and intermediate free radical in MeCN/benzene solutions. *J. Phys. Chem. A* **2003**, *107*, 3335−3340.
(15) Sabatani, E.; Nikol, H. D.; Gray, H. B.; Anson, F. C. Emission spectroscopy of $Ru(bpy)_2dppz^{2+}$ in Nafion. Probing the chemical environment in cast films. *J. Am. Chem. Soc.* **1996**, *118*, 1158−1163.
(16) Bertoncello, P.; Dennany, L.; Forster, R. J.; Unwin, P. R. Nafion−tris(2-2′-bipyridyl)ruthenium(II) ultrathin Langmuir−Schaefer films: Redox catalysis and electrochemiluminescent properties. *Anal. Chem.* **2007**, *79*, 7549−7553.
(17) Nakamura, K.; Kanazawa, K.; Kobayashi, N. Electrochemically controllable emission and coloration by using europium(III) complex and viologen derivatives. *Chem. Commun. (Cambridge, U. K.)* **2011**, *47*, 10064−10066.
(18) Zheng, L.; Chi, Y.; Shu, Q.; Dong, Y.; Zhang, L.; Chen, G. Electrochemiluminescent reaction between $Ru(bpy)_3^{2+}$ and oxygen in Nafion film. *J. Phys. Chem. C* **2009**, *113*, 20316−20321.
(19) Murray, R. W. *Molecular Design of Electrode Surfaces*; Wiley-Interscience: New York, 1992.
(20) Rajagopalan, R.; Aoki, A.; Heller, A. Effect of quaternization of the glucose oxidase "wiring" redox polymer on the maximum current densities of glucose electrodes. *J. Phys. Chem.* **1996**, *100*, 3719−3727.
(21) Tamaki, T.; Yamaguchi, T. High-surface-area three-dimensional biofuel cell electrode using redox-polymer-grafted carbon. *Ind. Eng. Chem. Res.* **2006**, *45*, 3050−3058.
(22) Ochi, Y.; Suzuki, M.; Imaoka, T.; Murata, M.; Nishihara, H.; Einaga, Y.; Yamamoto, K. Controlled storage of ferrocene derivatives as redox-active molecules in dendrimers. *J. Am. Chem. Soc.* **2010**, *132*, 5061−5069.
(23) Luk, Y.-Y.; Abbott, N. L. Surface-driven switching of liquid crystals using redox-active groups on electrodes. *Science* **2003**, *301*, 623−626.
(24) Daeneke, T.; Mozer, A. J.; Kwon, T.-H.; Duffy, N. W.; Holmes, A. B.; Bach, U.; Spiccia, L. Dye regeneration and charge recombination in dye-sensitized solar cells with ferrocene derivatives as redox mediators. *Energy Environ. Sci.* **2012**, *5*, 7090−7099.
(25) Su, C.; Ye, Y.; Xu, L.; Zhang, C. Synthesis and charge−discharge properties of a ferrocene-containing polytriphenylamine derivative as the cathode of a lithium ion battery. *J. Mater. Chem.* **2012**, *22*, 22658−22662.
(26) Nicolas, M.; Fabre, B.; Chapuzet, J. M.; Lessard, J.; Simonet, J. Boronic ester-substituted triphenylamines as new Lewis base-sensitive redox receptors. *J. Electroanal. Chem.* **2000**, *482*, 211−216.
(27) Choi, W.; Harada, D.; Oyaizu, K.; Nishide, H. Aqueous electrochemistry of poly(vinylanthraquinone) for anode-active materials in high-density and rechargeable polymer/air batteries. *J. Am. Chem. Soc.* **2011**, *133*, 19839−19843.
(28) Xu, W.; Read, A.; Koech, P. K.; Hu, D.; Wang, C.; Xiao, J.; Padmaperma, A. B.; Graff, G. L.; Liu, J.; Zhang, J.-G. Factors affecting the battery performance of anthraquinone-based organic cathode materials. *J. Mater. Chem.* **2012**, *22*, 4032−4039.
(29) Sano, N.; Tomita, W.; Hara, S.; Min, C.-M.; Lee, J.-S.; Oyaizu, K.; Nishide, H. Polyviologen hydrogel with high-rate capability for anodes toward an aqueous electrolyte-type and organic-based rechargeable device. *ACS Appl. Mater. Interfaces* **2013**, *5*, 1355−1361.
(30) Sen, S.; Saraidaridis, J.; Kim, S. Y.; Palmore, G. T. R. Viologens as charge carriers in a polymer-based battery anode. *ACS Appl. Mater. Interfaces* **2013**, *5*, 7825−7830.
(31) Zhou, H.; Yang, W.; Sun, C. Amperometric sulfite sensor based on multiwalled carbon nanotubes/ferrocene-branched chitosan composites. *Talanta* **2008**, *77*, 366−371.
(32) Oyaizu, K.; Ando, Y.; Konishi, H.; Nishide, H. Nernstian adsorbate-like bulk layer of organic radical polymers for high-density charge storage purposes. *J. Am. Chem. Soc.* **2008**, *130*, 14459−14461.
(33) Hyakutake, T.; Park, J. Y.; Yonekuta, Y.; Oyaizu, K.; Nishide, H.; Advincula, R. Nanolithographic patterning *via* electrochemical oxidation of stable poly(nitroxide radical)s to poly(oxoammonium salt)s. *J. Mater. Chem.* **2010**, *20*, 9616−9618.
(34) Buhrmester, C.; Moshurchak, L. M.; Wang, R. L.; Dahn, J. R. The use of 2,2,6,6-tetramethylpiperinyl-oxides and derivatives for redox shuttle additives in Li-ion cells. *J. Electrochem. Soc.* **2006**, *153*, A1800−A1804.
(35) Koshika, K.; Chikushi, N.; Sano, N.; Oyaizu, K.; Nishide, H. A TEMPO-substituted polyacrylamide as a new cathode material: An organic rechargeable device composed of polymer electrodes and aqueous electrolyte. *Green Chem.* **2010**, *12*, 1573−1575.
(36) Grampp, G.; Rasmussen, K. Solvent dynamical effects on the electron self-exchange rate of the $TEMPO^{\bullet}/TEMPO^{+}$ couple (TEMPO = 2,2,6,6-tetramethyl-1-piperidinyloxy radical). *Phys. Chem. Chem. Phys.* **2002**, *4*, 5546−5549.
(37) Endo, T.; Takuma, K.; Takata, T.; Hirose, C. Synthesis and polymerization of 4-(glycidyloxy)-2,2,6,6-tetramethylpiperidine-1-oxyl. *Macromolecules (Washington, DC, U. S.)* **1993**, *26*, 3227−3229.
(38) Nakahara, K.; Oyaizu, K.; Nishide, H. Electrolyte anion-assisted charge transportation in poly(oxoammoniumcation/nitroxyl radical) redox gels. *J. Mater. Chem.* **2012**, *22*, 13669−13673.
(39) Oyaizu, K.; Kawamoto, T.; Suga, T.; Nishide, N. Synthesis and charge transport properties of redox-active nitroxide polyethers with large site density. *Macromolecules (Washington, DC, U. S.)* **2010**, *43*, 10382−10389.
(40) Oyaizu, K.; Suga, T.; Yoshimura, K.; Nishide, H. Synthesis and characterization of radical-bearing polyethers as an electrode-active material for organic secondary batteries. *Macromolecules (Washington, DC, U. S.)* **2008**, *41*, 6646−6652.
(41) Yonekuta, Y.; Susuki, K.; Oyaizu, K.; Honda, K.; Nishide, H. Battery-inspired, nonvolatile, and rewritable memory architecture: A radical polymer-based organic device. *J. Am. Chem. Soc.* **2007**, *129*, 14128−14129.
(42) Finklea, H. O.; Haddox, R. M. Coupled electron/proton transfer of galvinol attached to SAMs on gold electrodes. *Phys. Chem. Chem. Phys.* **2001**, *3*, 3431−3436.
(43) Suga, T.; Sugita, S.; Ohshiro, H.; Oyaizu, K.; Nishide, H. p- and n-Type bipolar redox-active radical polymer: Toward totally organic polymer-based rechargeable devices with variable configuration. *Adv. Mater. (Weinheim, Ger.)* **2011**, *23*, 751−754.
(44) Sukegawa, T.; Kai, A.; Oyaizu, K.; Nishide, H. Synthesis of pendant nitronyl nitroxide radical-containing poly(norbornene)s as ambipolar electrode-active materials. *Macromolecules (Washington, DC, U. S.)* **2013**, *46*, 1361−1367.

(45) Koshika, K.; Sano, N.; Oyaizu, K.; Nishide, H. An ultrafast chargeable polymer electrode based on the combination of nitroxide radical and aqueous electrolyte. *Chem. Commun. (Cambridge, U. K.)* **2009**, 836−838.
(46) Suga, T.; Ohshiro, H.; Sugita, S.; Oyaizu, K.; Nishide, H. Emerging n-type redox-active radical polymer for a totally organic polymer-based rechargeable battery. *Adv. Mater. (Weinheim, Ger.)* **2009**, *21*, 1627−1630.
(47) Nesvadba, P.; Bugnon, L.; Maire, P.; Novak, P. Synthesis of a novel spirobisnitroxide polymer and its evaluation in an organic radical battery. *Chem. Mater.* **2010**, *22*, 783−788.
(48) Suga, T.; Konishi, H.; Nishide, H. Photocrosslinked nitroxide polymer cathode-active materials for application in an organic-based paper battery. *Chem. Commun. (Cambridge, U. K.)* **2007**, 1730−1732.
(49) Dalton, E. F.; Murray, R. W. Viologen(2+/l+) and viologen(1+/0) electron-self-exchange reactions in a redox polymer. *J. Phys. Chem.* **1991**, *95*, 6383−6389.
(50) Bockman, T. M.; Kochi, J. K. Isolation and oxidation−reduction of methylviologen cation radicals. Novel disproportionation in charge-transfer salts by X-ray crystallography. *J. Org. Chem.* **1990**, *55*, 4127−4135.
(51) Yonekuta, Y.; Oyaizu, K.; Nishide, H. Structural implication of oxoammonium cations for reversible organic one-electron redox reaction to nitroxide radicals. *Chem. Lett.* **2007**, *36*, 866−867.
(52) Pickup, P. G.; Murray, R. W. Redox conduction in mixed-valent polymers. *J. Am. Chem. Soc.* **1983**, *105*, 4510−4514.
(53) Saveant, J. M. Electron hopping between fixed sites "diffusion" and "migration" in counter-ion conservative redox membranes at steady state. *J. Electroanal. Chem.* **1988**, *242*, 1−21.
(54) Cheng, C. H. W.; Lonergan, M. C. A conjugated polymer pn junction. *J. Am. Chem. Soc.* **2004**, *126*, 10536−10537.
(55) Cayre, O. J.; Chang, S. T.; Velev, O. D. Polyelectrolyte diode: Nonlinear current response of a junction between aqueous ionic gels. *J. Am. Chem. Soc.* **2007**, *129*, 10801−10806.
(56) Koo, H.-J.; Chang, S. T.; Velev, O. D. Ion-current diode with aqueous Gel/SiO_2 nanofilm interfaces. *Small* **2010**, *6*, 1393−1397.
(57) Robinson, S. G.; Johnston, D. H.; Weber, C. D.; Lonergan, M. C. Polyelectrolyte-mediated electrochemical fabrication of a polyacetylene p−n junction. *Chem. Mater.* **2010**, *22*, 241−246.
(58) Pickup, P. G.; Leidner, C. R.; Denisevich, P.; Murray, R. W. Bilayer electrodes: Theory and experiment for electron trapping reactions at the interface between two redox polymer films. *J. Electroanal. Chem.* **1984**, *164*, 39−61.
(59) Pickup, P. G.; Kutner, W.; Leidner, C. R.; Murray, R. W. Redox conduction in single and bilayer films of redox polymer. *J. Am. Chem. Soc.* **1984**, *106*, 1991−1998.